

Kinematics of plaice, *Pleuronectes platessa*, and cod, *Gadus morhua*, swimming near the bottom

Paul W. Webb*

*School of Natural Resources and Environment and Department of Ecology and Evolutionary Biology,
University of Michigan, Ann Arbor, MI 48109-1119, USA*

*e-mail: pwebb@umich.edu

Accepted 24 April 2002

Summary

The kinematics of plaice (*Pleuronectes platessa*, $L=22.1$ cm) and cod (*Gadus morhua*, $L=25.0$ cm, where L is total fish length) swimming at various speeds at the bottom and lifted to heights, h , of 10, 50 and 100 mm by a thin-wire grid were measured. For cod, tailbeat frequency, amplitude, body and fin span and propulsive wavelength were unaffected by h and varied with speed as described for fusiform pelagic species. In contrast, the kinematics of plaice was affected by h . Body and fin spans and propulsive wavelength were independent of swimming speed and h . Tailbeat amplitude was independent of swimming speed, but averaged 1.5 cm at $h=0$ and 2.5 cm at $h \geq 10$ mm. Plaice tailbeat frequency increased with swimming speed for fish at the bottom but was independent of swimming speed at $h=10, 50$ and 100 mm, averaging 4.6, 6.0 and 5.8 Hz respectively. Total mechanical power, P , produced by propulsive movements calculated from the bulk-momentum form of elongated slender-body theory was similar for cod and plaice swimming at the bottom but, at $h \geq 10$ mm, P for plaice

was larger than that for cod. Plaice support their weight in water by swimming at a small tilt angle. The small changes in swimming kinematics with swimming speed are attributed to decreasing induced power costs to support the weight as speed increases. The contribution of the tail to power output increased monotonically with the tail gap/span ratio, z/B , for $z/B=0.23$ ($h=0$ mm) to $z/B=1.1$ ($h=50$ mm). The smaller tailbeat amplitude of the tail decreased both z/B and the power output for plaice swimming at the bottom. For the maximum body and fin span of plaice, the contribution to power output increased for local z/B values of 0.044 ($h=0$ mm) to 0.1 ($h=10$ mm) and declined somewhat at larger values of z/B . The smaller effect of the bottom on power output of the large-span anterior body sections may result from the resorption of much of the upstream wake at the re-entrant downstream tail.

Key words: kinematics, plaice, *Pleuronectes platessa*, cod, *Gadus morhua*, swimming, power, tailbeat amplitude.

Introduction

Most fishes live in cluttered habitats characterized by structures such as surfaces, struts (e.g. large woody debris) and protuberances (e.g. boulders). These habitats are typically productive and support a rich fauna of benthic fishes (Moyle and Cech, 1996). Many benthic fishes are flattened in the plane of the substratum and negatively buoyant, especially when there are currents for which these features facilitate station-holding (Arnold and Weihs, 1978). The most flattened groups are found among the pleuronectiform flatfishes, batoid rays and more ray-like selachians. These fishes also have large body spans, probably to help maintain body volume in spite of body flattening.

The swimming kinematics of highly flattened benthic fishes differs from that of their more fusiform relatives. The amplitude of body motions tends to be large over a greater portion of the propulsor, with plaice being more anguilliform and rays giving their name to swimming with large-amplitude undulations of the pectoral fins in the rajiform mode (Breder,

1926; Rosenberger, 2001). Human-engineered vehicles and animals moving close to a solid surface can reduce thrust requirements and increase efficiency as a result of interactions between the wake and the surface (ground effect) (Reid, 1932; Blake, 1979, 1983a,b; Lighthill, 1979; Webb, 1993). This hydrodynamic ground effect does not affect fast-start performance (Webb, 1981), but continuous swimmers do benefit (Blake, 1979; Webb, 1993). The ground effect for axial undulatory swimming fish decreases rapidly with height, being reduced by up to 95% at a gap/span ratio of 1, and becoming very small, essentially negligible, at a value of 2 (Webb, 1993). For rigid bodies, ground effects reach zero at a gap/span ratio of 3 (Reid, 1932; Blake, 1979, 1983b; Lighthill, 1979).

To assess the effects of a nearby surface on the swimming of benthic fishes, observations were made on plaice (*Pleuronectes platessa*) and cod (*Gadus morhua*) swimming at various heights above the bottom. This study focuses on plaice, a benthic species with a compressed body that swims on its

side with propulsive motions normal to the substratum. As a result, plaice could derive substantial advantage from the ground effect, and swimming motions, especially tailbeat frequency, were expected to vary with height. Observations were also made on cod. Cod is a benthopelagic species that swims with a vertical posture, making swimming movements parallel to the substratum. Cod would be expected to derive little benefit from swimming near the bottom, so that swimming kinematics should be unaffected by swimming height above the bottom. Cod-like swimmers have been extensively studied and are included as a check that changes in the swimming motions of plaice at various heights above the substratum can be attributed to ground effects.

Materials and methods

Fish

Fish, plaice (*Pleuronectes platessa*) and cod (*Gadus morhua*), were caught near Lowestoft (England) using beam trawls. They were held in 1200l tanks, continuously aerated and flushed with filtered sea water at 15 °C for 4–6 weeks before the start of experiments. Fish were fed on chopped lugworm, mackerel and herring.

Apparatus

Swimming kinematics was observed in a flume described in detail by Arnold (1969). Briefly, the flume was constructed from 1.25 cm thick Perspex. It was approximately 6 m long, with a 0.3 m × 0.3 m cross section. Water entered *via* a contraction cone. The first 1.8 m of the flume was an entry section, which was followed by an 1.8 m observation section. Nylon mesh screens delineated the observation section. A clear Plexiglas boat floated on the surface, 1 cm below the wall height, to eliminate surface waves. Cross-sectional flow profiles through the observation section have been shown to be rectilinear (Arnold, 1969; Webb, 1989). The final 1.8 m of the flume terminated at a gate. The height of the gate and the rate of water input upstream of the contraction cone were used to regulate flow velocity while keeping the water at the desired level. Free-stream flow velocity was continuously monitored using a MINFLOW meter 15 cm above the bottom immediately upstream of the observation section.

Swimming kinematics were recorded for fish swimming on the smooth bottom and over a grid of wires parallel to the flow lifting fish to heights, h , of 10, 50 and 100 mm above the bottom. The wires were strung on an aluminum frame with sides 1.0 cm square and 2 m long, with streamlined cross-pieces 0.624 cm thick at each end. Stainless-steel wires (0.01 mm diameter) were strung at 1.0 cm intervals along the cross-pieces and held under tension by turnbuckles at the downstream end of the grid. The frame for the grid extended beyond the end of the observation section, and the turnbuckles were beyond the downstream screen.

Swimming on a grid is not identical to swimming in the free stream at the same height because the wires cause some

retardation of flow across the surface. Wires were spaced at the maximum distance that prevented fish from passing easily through the grid. Actual downwash velocities are not known but, because much of the mass of plaice is supported by buoyancy in water, they are probably not large. A grid of wires with the same spacing normal to the flow in the flume showed a velocity loss at 5 cm s⁻¹ of less than 4%. Maximum streamwise velocity losses due to such a grid at higher flow rates were previously found to be up to 20% (Webb, 1989).

Gap/span ratio

Pleuronectiformes swim on their side. As a result, body and caudal fin motions are parallel to the ground. Therefore, thrust should be enhanced and rates of working reduced by the ground effect (Reid, 1932; Lighthill, 1979). Ground effects depend on the gap/span ratio, z/B , where z is the gap, the space between a solid surface and the thrust-producing body and fins, and B is span, equal to the depth of the body and fins for plaice and cod.

Fish propel themselves with flapping propulsors so that the gap varies through a propulsor cycle. The ground effect decreases monotonically to an asymptote with increasing z/B . To take into account this non-linear variation, Webb (1993) used the geometric mean gap for fish swimming near walls. This mean was calculated from limits when a propulsive element was closest and most distant from a solid surface. For the present experiments, this leads to:

$$z = (z_{1,\text{bottom}} \times z_{2,\text{bottom}} \times z_{1,\text{boat}} \times z_{2,\text{boat}})^{0.25}, \quad (1)$$

where $z_{1,\text{bottom}}$ is the distance above the bottom (ground) at one extreme of the tailbeat and $z_{2,\text{bottom}}$ is the distance above the bottom at the other extreme, $z_{1,\text{boat}}$ is the distance below the boat at one extreme of the tailbeat and $z_{2,\text{boat}}$ is the distance below the boat at the other extreme.

In addition, the ground effect is small at $z/B \approx 2$ for axial undulatory swimmers and falls to zero at z/B of 3 for rigid bodies (Reid, 1932; Blake, 1979, 1983b; Lighthill, 1979). Values for z were used only when z/B between the propulsor and a solid surface was ≤ 3 , with the exponent of equation 1 reduced accordingly.

The tail contacts the grid or bottom once in each tailbeat cycle. At this point, $z_{1,\text{bottom}} = h$. At the other extreme of the tailbeat amplitude, $z_{2,\text{bottom}} = h + H$, where H is the amplitude of a beat. For the special case of $h = 0$, $z_{1,\text{bottom}}$ is zero and mean $z_{\text{bottom}} = H^{0.5}$. The total depth available was limited to 29 cm, so that $z_{1,\text{boat}} = 29 - h$, and $z_{2,\text{boat}} = 29 - h - H$, with the units being in centimeters.

Gap/span ratio was calculated similarly for cod, with distances to the walls replacing the distance to the bottom and the boat.

Experimental procedure

Individual fish were placed in the observation section and left overnight at a free-stream velocity of approximately 5 cm s⁻¹. The following morning, the flow velocity was

Table 1. Morphometrics of the plaice and cod used in experiments

	Plaice	Cod
Total length (cm)	22.1±0.9	25.0±1.4
Mass in air (g)	96.629±10.691	126.513±20.134
Weight in sea water (g)	4.281±0.400	0.154±0.002
Density (g cm ⁻³)	1.0728±0.0031	1.0263±0.0002
Maximum span, B_{\max} (cm)	12.2±0.5	7.0±0.6
N	10	9

Values are means ± 2 S.E.M.

increased in increments of approximately 5 cm s⁻¹ (Δu) every 10 min (Δt). An experiment was terminated when a fish was unable to swim off the downstream screen delineating the observation section. This 10-min critical swimming speed (u_{crit}) was calculated as described by Brett (1964): 10-min $u_{\text{crit}} = u_p + \Delta u t / \Delta t$, where u_p is the penultimate speed before failure at which fish swam for the full 10 min. The test temperature was 15 °C.

At the end of an experiment, fish were killed with 3 ml l⁻¹ phenoxyethanol. Mass was measured to within 1 mg in air. Each fish was also weighed in sea water (density 1.025 g cm⁻³), from which the density of each fish was calculated. Fish were suspended by a thread from a beam attached to the balance pan. The fish was immersed in a bucket of sea water. Measured weight was corrected for the weight of the beam and thread. Total length was measured to within 0.1 cm. These measurements are summarized in Table 1. The maximum or potential depth of the body and extended fins was measured to within 0.1 cm at 22 points equidistant along the centerline of cod and at 13 points along that of plaice. Fewer data points were required to characterize the simple body shape of plaice.

Throughout each experiment, fish were videotaped simultaneously in the horizontal plane and in the vertical plane *via* a mirror placed at 45° above the observation section. Sequences were analyzed that fulfilled the following conditions: (i) swimming was steady, defined as less than 10%, usually less than 5%, variation in speed between tailbeats, (ii) fish swam in the center of the flume, defined as the distances to each wall at the limits of tailbeat amplitudes varying by less than 10%, usually less than 5%, and (iii) for at least 10 complete tailbeats. Videotape was analyzed field-by-field (50 Hz), and body outlines were digitized through a tailbeat cycle. Tailbeat frequency was determined from the period taken by the tail to move from one extreme lateral position and back to the original position. The period was also measured for each half-beat. Tailbeat amplitude was measured as the distance between the maximum lateral displacements of the tip of the tail during a complete tailbeat and a half-tailbeat. The span of the trailing edges of cod was measured (i) at the tail, (ii) at the second dorsal and first ventral fin and (iii) at the third dorsal fin/second ventral fin, and for plaice (i) at the tail and (ii) at the maximum span of

the body and median fins. The posterior speed of the propulsive wave was measured from successive positions of wave crests travelling along the body. The length of the propulsive wave was determined by dividing this wave speed by the tailbeat frequency.

The angle subtended by the body and the horizontal plane is the tilt angle (He and Wardle, 1986; Webb, 1993). The midline along the body of the swimming fish was determined as the central point between body outlines at maximum amplitude. Digitized outlines were superimposed, and a linear regression was fitted to amplitude limits along the body. The tilt angle was measured as the slope of this line.

Statistical analyses

Multiple comparisons among various swimming parameters were compared using analysis of variance (ANOVA) followed by Tukey's multiple-comparison tests to locate significant differences. Relationships between kinematic parameters and speed were examined using best-fit linear regressions. Comparisons between pairs of data sets were made using Student's *t*-tests. Computations were made using SYSTAT (Wilkinson, 1987). Significant differences are declared for $\alpha \leq 0.05$. Descriptive statistics are reported as means ± 2 S.E.M. (see Sokal, 1995).

Results

Limits of swimming speeds

Cod and plaice held station on the bottom without swimming at low current speeds, as described previously (Arnold, 1969; Arnold and Weihs, 1978; Webb, 1989). Cod began swimming at an average speed of 9 cm s⁻¹ (Fig. 1). These swimming speeds were independent of h (ANOVA, $P > 0.9$). Plaice began swimming at current speeds of 15–25 cm s⁻¹. Swimming speeds on the grid at different values of h were not significantly different from each other ($P > 0.8$). As found elsewhere (Webb, 1989), swimming speed was higher for plaice at the bottom compared with the average for the grids (*t*-test, $P < 0.01$), and plaice swimming speeds were significantly larger than those of cod (ANOVA, $P < 0.05$).

The 10-min u_{crit} of cod was 57 cm s⁻¹, similar to that of 54 cm s⁻¹ for plaice swimming at the bottom (*t*-test, $P > 0.8$). The 10-min u_{crit} of plaice was unaffected by height for $h \geq 10$ mm, averaging 46 cm s⁻¹ (ANOVA, $P < 0.08$). The mean 10-min u_{crit} of these fish was significantly lower than that for plaice swimming at the bottom (*t*-test, $P < 0.04$).

Swimming mode

Both species swam by passing an undulatory wave along the body (Fig. 2). The wavelength of the propulsive wave, λ , was independent of both speed and swimming height (ANOVA, $P > 0.9$). Wavelengths averaged 16.4±0.2 cm ($N=259$) (0.74 L , where L is fish total length) for plaice and 23.3±5.7 cm ($N=158$) (0.93 L) for cod. Plaice swimming was therefore more anguilliform than that of cod.

Specific amplitude (H/L) of cod varied along the body

length (Figs 2, 3A), as described for other subcarangiform swimmers (Bainbridge, 1963; Webb, 1988, 1992). Values decreased rostrally from a maximum of $0.16L$ at the trailing edge to a minimum of $0.03L$ at a distance of approximately $0.3L$ from the nose. Specific amplitude then increased over the head to $0.04L$ at the nose.

The distribution of specific amplitude along the body length of plaice differed from that of cod. Plaice specific amplitudes decreased continuously from a maximum at the trailing edge to a minimum at the nose (Fig. 3B). This pattern, lacking a minimum behind the head, has been described for eel *Anguilla anguilla* (Gray, 1933) and tiger musky *Esox* sp. (Webb, 1988) in association with a more anguilliform mode of swimming.

In addition, specific amplitude increased at a lower rate over the posterior of the body of plaice compared with cod (Figs 2, 3A,B). This is characteristic of more anguilliform species compared with more carangiform species (Breder, 1926).

The weight of cod in water, averaging 0.15 g, was 0.1% of the weight in air (Table 1). Thus, cod were essentially neutrally buoyant, and these fish swam with a horizontal posture at all speeds and at all heights. Plaice were more dense than sea water, supporting a weight of 4 g, approximately 4.4% of the weight in air (Table 1). There were no significant differences in the duration or amplitude of tailbeats towards and away from the bottom at any value of h (ANOVA, $P>0.1$). However, plaice swam at positive tilt

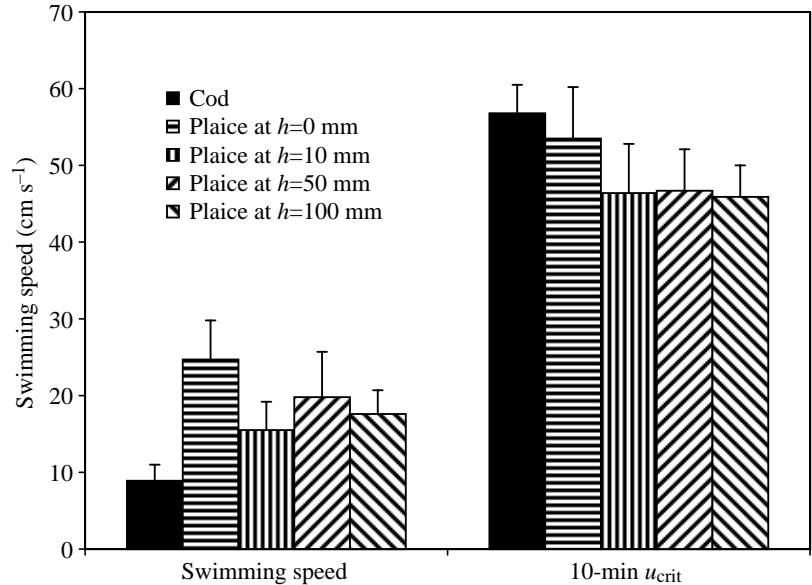


Fig. 1. Swimming speeds at which fish began to swim and 10-min critical swimming speeds (u_{crit}) for cod, and for plaice at various heights, h , above the bottom. Values are means + 2 S.E.M. Sample sizes are given in Table 1.

angles, as shown by the head-up postures of the plaice centerline tracings in Fig. 2. These angles were variable, as observed elsewhere (He and Wardle, 1986; Webb, 1993; Wilga and Lauder, 1999, 2000, 2001). Although there was a tendency for angles to decrease with increasing speed, the trend was not significant; in addition, no relationship was found between tilt angles and h (ANOVA, $P>0.4$). The overall tilt angle was $4\pm 3^\circ$ ($N=259$), and the 95% confidence interval around the mean did not include zero.

Kinematics

Tailbeat frequency, F , and tailbeat amplitude, H , of cod were not affected by swimming height above the bottom (ANOVA, $P>0.1$). Data for fish swimming at various values of h were therefore pooled (Fig. 4A). F increased linearly with speed from approximately 1.8 Hz at 10 cm s^{-1} to 3.9 Hz at 55 cm s^{-1} . H also increased linearly with speed from 2.9 to 4.7 cm (0.12 and $0.19L$, respectively) over the same range of speeds so that $H=(2.5\pm 0.2)+(0.039\pm 0.007)u$, $r^2=0.55$, $P<0.001$.

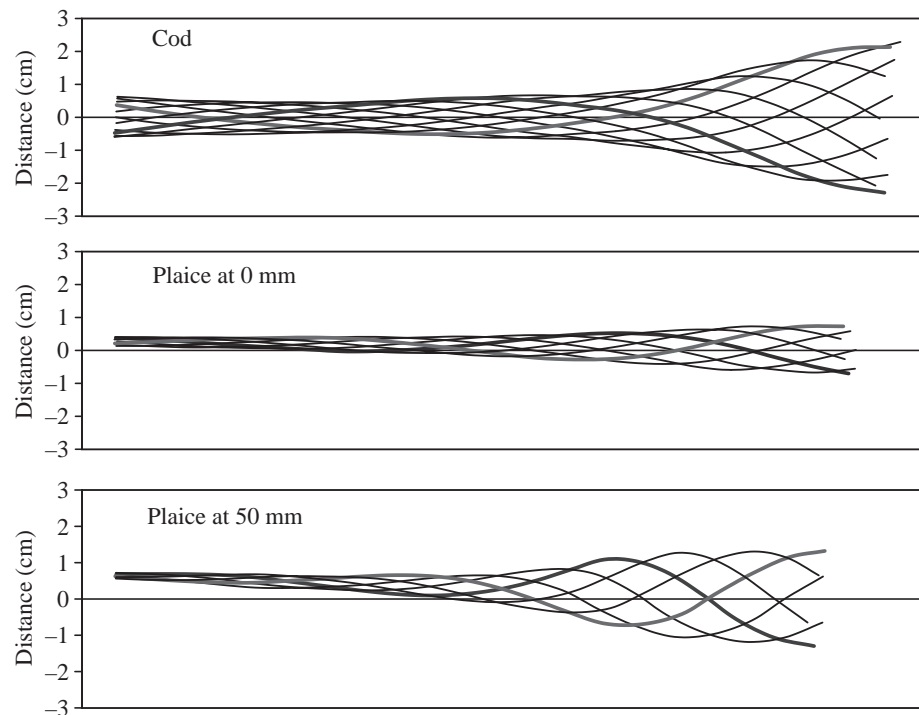


Fig. 2. Tracings of the centerlines of the body of cod and plaice swimming at 35 cm s^{-1} . Observations are shown for plaice swimming at the ground (0 mm) and at a height of 50 mm. Centerlines are shown for 1/30 s intervals.

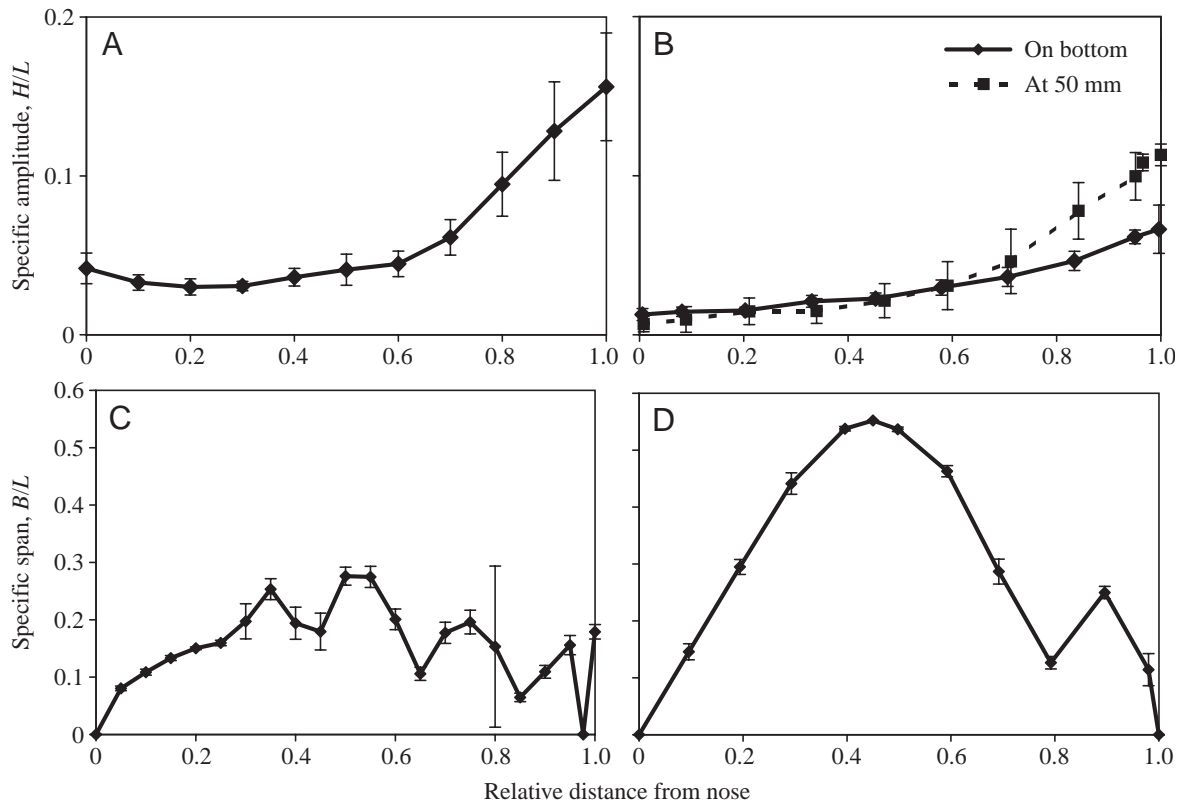


Fig. 3. The distribution of amplitude, H , and span, B , along the length of swimming cod ($N=9$) and plaice ($N=10$). (A) Specific amplitudes of cod at all values of h , (B) specific amplitudes of plaice, (C) specific spans of cod and (D) specific spans of plaice. Amplitudes, and the span of the body and fins, are normalized to total body length (L). Locations along the body length are normalized to total length as relative position along the body. Data in B are shown only for plaice swimming at the bottom and at a height of 50 mm for clarity. Values are means \pm 2 S.E.M.

These motions are comparable with those of other species swimming in the water column when tailbeat frequency is the major kinematic variable modulated with swimming speed. Amplitude also increases with speed for some species, but not others (Webb, 1975; Videler, 1993; Webber et al., 2001).

For plaice, F for fish swimming at the bottom increased with speed from an average of 3.5 Hz at 25 cm s^{-1} to 4.7 Hz at 55 cm s^{-1} (Fig. 4A). At $h=10 \text{ mm}$, there was some tendency for F to increase with speed, but the relationship was not significant ($P=0.051$). Therefore, F was independent of swimming speed, averaging 4.6, 6.0 and 5.8 Hz at 10, 50 and 100 mm respectively (Fig. 4B). The tailbeat frequencies of plaice swimming above the bottom at all speeds were significantly greater than those of cod (ANOVA, $P<0.01$).

The tailbeat amplitudes of plaice (Fig. 4C) were independent of swimming speed at all heights ($P>0.2$). However, H was smallest at 1.5 cm ($0.07L$) for plaice swimming at the bottom, compared with amplitudes of 2.4–2.6 cm (0.11 – $0.12L$) at $h\geq 10 \text{ mm}$ (Fig. 4C). The tailbeat amplitudes of plaice swimming at $h\geq 10 \text{ mm}$ were not significantly different from each other ($P>0.3$) but were significantly greater than for plaice swimming at the bottom ($P<0.001$).

For plaice, amplitude distribution along the body was affected by h (Figs 2, 3B). Specific amplitudes of the body over

the anterior $0.7L$ of the body of plaice were independent of h , and those over the posterior 30% differed for fish at 0 and $\geq 10 \text{ mm}$ (ANOVA, $P>0.2$). The amplitudes at 10, 50 and 100 mm were significantly larger than those at 0 mm ($P<0.05$). For example, the tail amplitude averaged $0.07L$ for plaice swimming at the bottom and $0.11L$ for plaice swimming at 50 mm.

Span

The potential span, expressed as specific span, B/L (Fig. 3C,D), varied with position along the length of the body of both species. Variations for cod followed the locations of the median fins (Fig. 3C). The maximum span of $0.28L$ for cod occurred at $0.5L$ along the body, associated with the second dorsal and first ventral fin. The maximum span exceeded that of the third dorsal fin/second ventral fin of $0.2L$ at $0.75L$ along the body, which in turn exceeded the maximum span at the caudal fin of $0.16L$. As a result, upstream median fins could shed an outboard portion of the vortex sheet which will not be absorbed at the leading edge of the downstream fins. Such fins could contribute to mean thrust production (Lighthill, 1975).

For plaice, the maximum specific span of $0.55L$ occurred at $0.45L$ from the nose (Fig. 3D). Span initially decreased continuously from this maximum over the posterior of the body, before increasing to $0.25L$ at the caudal fin. The trailing edge

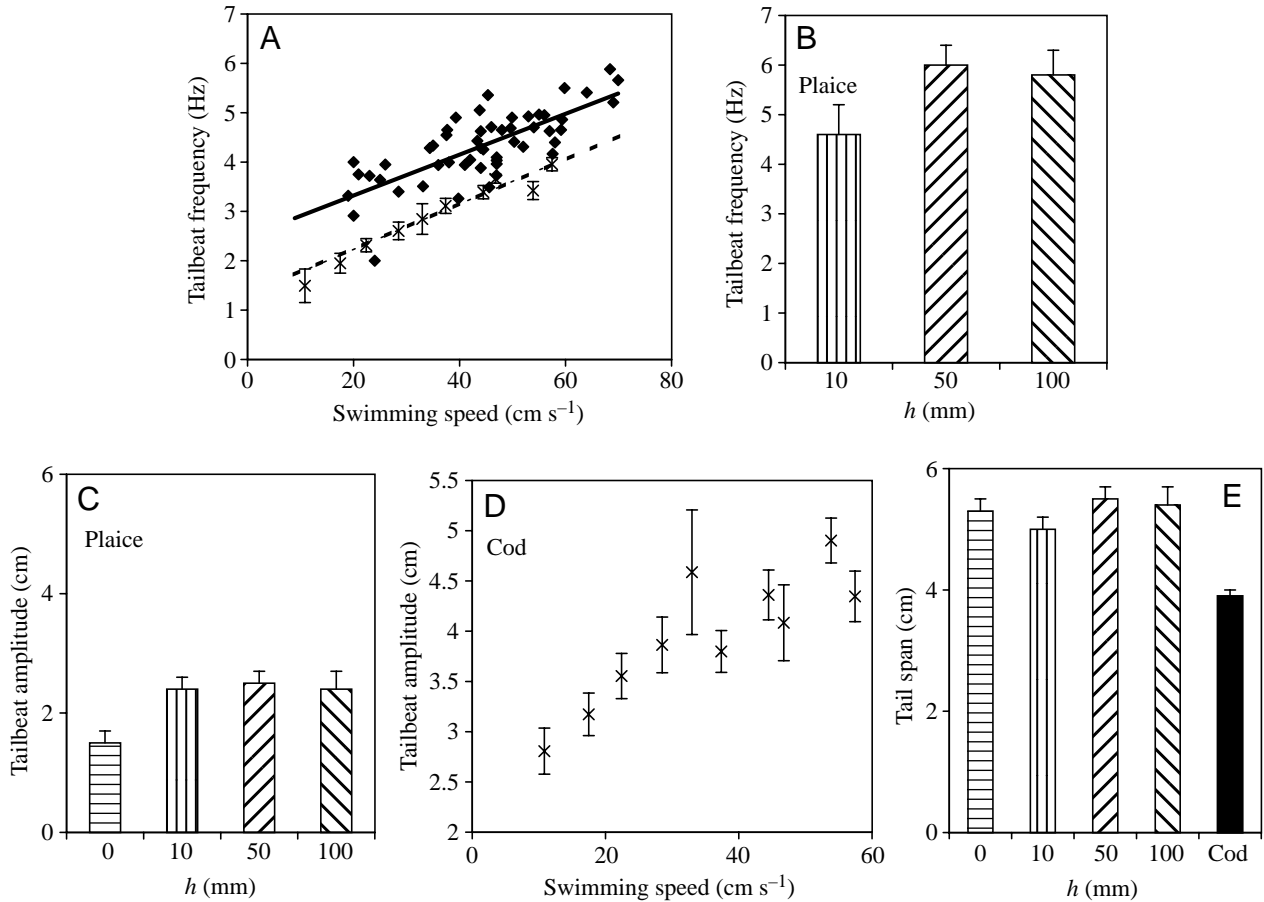


Fig. 4. Relationships between the tailbeat characteristics and swimming speed for cod and plaice swimming at various heights, h , above the bottom. (A) Tailbeat frequencies (F) of plaice (filled diamonds) at $h=0$ mm and the best-fit linear regression (solid line); $F=(2.46\pm 0.60)+(0.041\pm 0.012)u$, $r^2=0.58$, $P=0.003$, $N=62$. Mean tailbeat frequencies of cod (crosses; means ± 2 S.E.M.), averaged for 5 cm s^{-1} speed bands, for clarity, for all values of h combined. The best-fit linear regression (dotted line) is described by: $F=(1.31\pm 0.17)+(0.046\pm 0.005)u$, $r^2=0.72$, $P=0.003$, $N=158$. (B) Tailbeat frequencies of plaice (means ± 2 S.E.M.) were independent of speed for $h\geq 10$ mm. Values averaged for all speeds are shown for $h=10$ mm ($N=72$), 50 mm ($N=64$) and 100 mm ($N=71$). (C) Tailbeat amplitudes of plaice (means \pm S.E.M.), which were independent of speed for all heights, are shown for different values of h . (D) Mean tailbeat amplitudes of cod (crosses) (means ± 2 S.E.M.) are shown, averaged for 5 cm s^{-1} speed bins, for clarity, for all values of h combined. (E) Values for the span (B) of the caudal fin. Values averaged over all speeds for cod and plaice at four different values of h are shown because B was independent of speed and h . Values are means ± 2 S.E.M.

of the caudal fin was convex so that the maximum tail span occurred at approximately $0.1L$ anterior to tip of the caudal fin.

Swimming tail spans, B , of cod and plaice were independent of speed and swimming height (Fig. 4E) (ANOVA, $P>0.09$). Overall mean tail span was 3.9 ± 0.1 cm ($N=257$) ($0.16L$) for cod, representing 89% of the potential depth. For plaice, swimming tail span averaged 5.2 ± 0.1 cm ($N=158$) ($0.24L$), which was not significantly different from the potential span. Although plaice had a smaller total length than cod, the tail spans of plaice were significantly larger (t -tests, $P<0.01$) than those of cod. Similar results were obtained for spans at other body locations, although these tended to be more variable than for the tail, especially for cod. Thus, the maximum span for cod averaged $90\pm 23\%$ of the potential span (Fig. 3C) at the second dorsal/first ventral fin, and $85\pm 21\%$ at the trailing edge of the third dorsal fin/second ventral fin. In contrast, the

maximum span of swimming plaice was $98\pm 10\%$ of the specific span (Fig. 3D).

Gap/span ratio

The span of propulsive sections of plaice did not vary with swimming speed. Gap/span ratios at a given position along the body were therefore independent of speed.

Cod were videotaped when swimming in the center of the flume. For all points along the body, $z/B>2$; at this value of z/B , ground effects are very small for axial undulatory swimmers (Webb, 1993). Therefore ground-effect interactions with the walls were considered negligible.

For plaice, z/B for the tail (z_{tail}/B) was varied from 0.23 at the bottom to 2.16 at $h=100$ mm (Table 2). At the position of maximum span, z/B_{max} was smaller, varying from 0.04 to 1 over the same range of h .

Table 2. Gap/span ratios for the tail and maximum span of plaice swimming at various heights above the bottom

Kinematic variable	Swimming on bottom	Swimming on grid		
		10 mm above bottom	50 mm above bottom	100 mm above bottom
Gap/span ratio for tail	0.231±0.020	0.372±0.013	1.11±0.029	2.16±0.018
Gap/span ratio for maximum span	0.044±0.020	0.099±0.013	0.443±0.029	0.98±0.018

Values are means ± 2 s.e.m., N=10.

Discussion

The goal of these experiments was to determine the consequences of swimming near the ground by benthic fishes, especially for plaice whose body shape and posture could provide substantial benefits from ground effects. In general, the swimming motions of cod were typical of other species swimming in the water column (Webb, 1975; Videler, 1993; Webber et al., 2001). Tailbeat frequency and amplitude varied with speed, especially the former. The span of the trailing edge and propulsive wavelength were constant. These were not affected by swimming height. Cod therefore derived no benefit from the ground effect.

As with cod, the trailing-edge span and propulsive wavelength of plaice were independent of speed. Tailbeat amplitudes of plaice were also independent of speed; such speed-independence is common among carangiform and subcarangiform swimmers (Webb, 1975; Videler, 1993; Webber et al., 2001). Relationships between tailbeat frequency and swimming speed of plaice were notably different from those of most swimmers. F increased with speed, as is typical of other fish, only when plaice were swimming at the bottom. For $h \geq 10$ mm, F was independent of speed.

Power

Interactions with the bottom by plaice are expected to affect rates of working, with substantial reductions as z/B decreases below 2 (Webb, 1993). Therefore, to evaluate better the effects of speed and height on swimming, rates of working were determined using a bulk-momentum hydromechanical model derived from elongated slender-body theory (Lighthill, 1975; Wu, 1977). The mean rate of working for an element, x , along the body, P_x , is:

$$P_x = MWwu, \quad (2)$$

where:

$$M = \rho_{\text{water}} \pi B_x^2 / 4, \quad (3)$$

$$W = \pi F_x H_x / \sqrt{2}, \quad (4)$$

$$w = W[1 - (u/c)], \quad (5)$$

and ρ_{water} is the density of sea water, M is added mass per unit length of an element, W is the mean lateral speed assuming sinusoidal motion, w is the velocity given to the water, B_x is the local span, F_x is the local tailbeat frequency, H_x is the local amplitude and c , the backward speed of the propulsive wave, is equal to $F\lambda$.

Momentum carried by upstream fins and sharp body edges

may be absorbed into the wake of a re-entrant downstream fin with no net effect on the mean rate of working, P . However, when the span of a body/fin element is greater than that of a downstream re-entrant fin, the non-re-entrant portion of the vortex sheet shed by the upstream fin contributes directly to P (Lighthill, 1975; Newman and Wu, 1973; Wu, 1977). Both cod and plaice have upstream fins with substantially larger spans than downstream fins. Therefore, for cod, P was calculated as the sum of P_x for the non-re-entrant portions of the second dorsal/first ventral fins, for the third dorsal/second ventral fins and for the tail (Webb, 1988, 1992).

Plaice lack discrete upstream fins. The contribution of the continuous non-re-entrant portion of the dorsal and anal fins was calculated for 1-cm long panels along the body length from B_{max} at $0.45L$ measured from the nose until body and fin span equaled the tail span at $0.7L$ (Fig. 3D). The non-re-entrant contributions from these sections were summed with the contribution from the tail to obtain P .

Swimming power, speed and kinematics

The swimming power for cod increased exponentially with swimming speed (Fig. 5), as described for other fishes swimming in the water column (Webb, 1975; Blake, 1983a; Videler, 1993). The swimming power of plaice at the bottom also increased with speed, but at lower rates than for cod

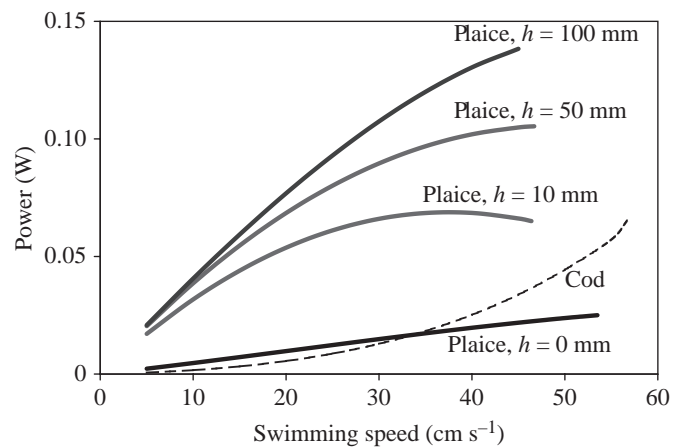


Fig. 5. The relationships between total mechanical power, P , and swimming speed for cod and for plaice swimming at heights, h , of 0, 10, 50 and 100 mm above the bottom. Although plaice only swam at current speeds >15 cm s $^{-1}$, the power curves have been extrapolated to lower speeds for comparison with cod.

(Fig. 5). Plaice at the bottom started swimming at a current speed of 25 cm s^{-1} and cruised up to 54 cm s^{-1} . At the lower end of this speed range, P was slightly larger than for cod (Fig. 5), but above 35 cm s^{-1} , plaice expended less mechanical power than cod. As h increased, so did P . For plaice swimming at $h \geq 10 \text{ mm}$, P was larger than that of cod over the whole range of cruising speeds. Thus, the mechanical power expended by plaice for continuous cruising was only comparable with that of cod when the plaice swam close to the bottom.

Part of the swimming power of plaice, the induced power, is used to generate lift and to support the weight of the fish in water. In birds, the necessity of supporting weight is associated with complex and asymmetrical wing motions on the upstroke and the downstroke (Norberg, 1990). No beat asymmetry was detectable in plaice. Another approach to balancing weight is to tilt, i.e. to swim or fly 'uphill'. Negatively buoyant fishes swim at low speeds with a positive, head-up tilt, as observed for plaice (He and Wardle, 1986; Wilga and Lauder, 1999, 2000, 2001).

Supporting weight dissipates energy as induced power (Hoerner, 1975; Anderson and Eberhardt, 2001). Because weight is independent of speed, a rapidly decreasing portion of the total force generated by a propulsor is required to support the weight. As a result, the associated induced drag decreases with speed. In the present experiments, this might be expected to be associated with a decrease in tilt angle with increasing speed, as observed for other fishes, but no significant decreases were observed for plaice. This may occur because plaice do not swim at the low speeds at which large changes in tilt angle occur. Thus, although a decrease in tilt would be anticipated, this would be small and difficult to identify given the usual variation in tilt angles (He and Wardle, 1986; Wilga and Lauder, 1999, 2000, 2001; Webb, 2002).

The effects of speed on induced power and that associated with translocation may explain the relative constancy in kinematic variables with speed of plaice swimming above the bottom. Kinematics and metabolic and mechanical rates of working have recently been reviewed for negatively buoyant swimmers, together with a thorough analysis of swimming for the brief squid *Lolliguncula brevis* (Bartol et al., 2001a,b). There is typically a shallow U-shaped relationship between power and speed. High swimming costs at low speeds are associated with large induced drag, while high costs at high speeds reflect energy costs for translocation. In contrast with other negatively buoyant swimmers, plaice avoid swimming at low speeds (Fig. 1). As a result, the rising part of the power curve at $h \geq 10 \text{ mm}$ at low speeds is avoided (Fig. 5) (Duthie, 1982; Bartol et al., 2001b).

When the U-shaped speed/power curve is shallow, the lack of variation in kinematics with speed is not surprising. In addition to the fin-beat frequencies of plaice swimming at $h \geq 0 \text{ mm}$, those of several rays, a benthic group swimming at the bottom (Rosenberger, 2001), and brief squid (Bartol et al., 2001b) are independent of swimming speed or even decrease with increasing speed (Bartol et al., 2001b). Thus, swimming patterns and power production are similar among negatively

buoyant swimmers and these, in turn, are similar to those for flying birds, bats and insects (Bartol et al., 2001a,b).

Swimming power, height and kinematics

Swimming height had no effect on the kinematics of cod, while plaice swimming was affected. At $h \geq 10 \text{ mm}$, the tailbeat frequencies of plaice were independent of speed (Fig. 4A,B). As h increased from 0 to $\geq 10 \text{ mm}$, tailbeat amplitude increased from $0.06L$ to $0.11L$ (Fig. 4B). The net effect of these changes in swimming patterns was an increase in the rate of working as h increased (Fig. 5). When expressed in terms of the gap/span ratio, P_x for the tail tended to increase monotonically with z/B to a maximum at 1.1 ($h=50 \text{ mm}$) (Fig. 6A). This is similar to the pattern seen for interactions with a wall in trout *Oncorhynchus mykiss* (Webb, 1993). A slight decrease in P_x is suggested at larger values of z/B but, given the normal variation in the input data, little importance can be attached to this decrease.

The relationships between z/B and power are consistent with observations in other systems that small changes in z/B when this ratio is small have larger effects on power output. This may explain the lower amplitude of the tailbeat of plaice swimming at the bottom compared with swimming at $h \geq 10 \text{ mm}$. For plaice swimming at the bottom, z/B averaged 0.23 (Table 2). If the tail amplitude were the same on the bottom as at

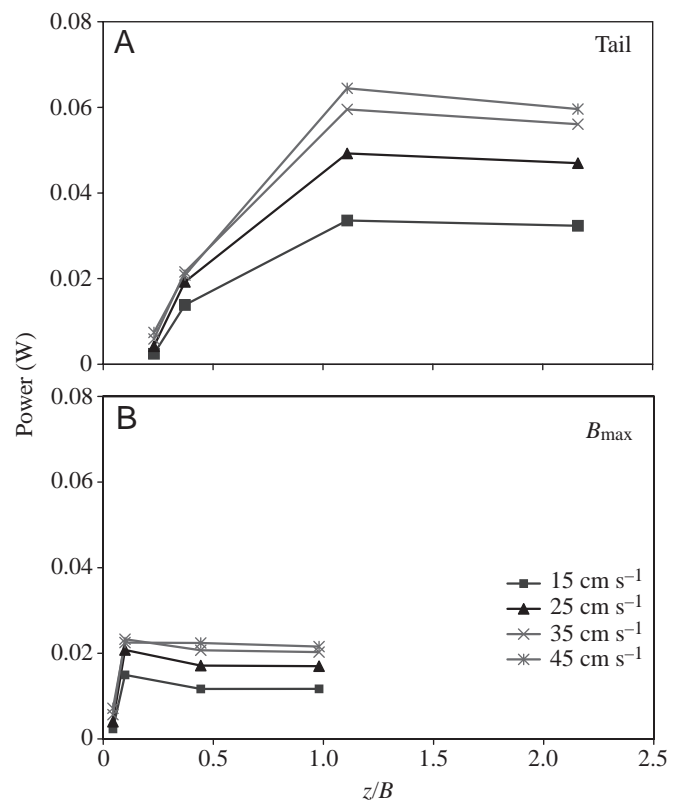


Fig. 6. The relationship between the gap/span ratio (z/B) and total mechanical power for plaice swimming at speeds of 5–45 cm s^{-1} . Results are shown for (A) the tail and (B) the non-re-entrant portion of the body and median fins at the maximum span, B_{max} .

$h \geq 10$ mm, z/B would increase to 0.3. Plaice would then require approximately twice as much power to swim (Fig. 6A).

For B_{\max} , P_x increased as z/B_{\max} increased from 0.04 ($h=0$ mm) to 0.1 ($h=10$ mm) but then decreased at larger values of z/B (Fig. 6B). The decrease in P_x at only the smallest values of z/B may occur because much of the upstream wake is absorbed at the leading edge of re-entrant downstream fins, with insufficient time to develop and interact with the bottom.

Nevertheless, the relationship between power and z/B_{\max} is such that there would be an advantage to decreasing amplitude at maximum span, as for the tail. Mean amplitudes were lower at B_{\max} for plaice at the bottom (Fig. 6B), but the difference is not significant. Other unknown factors may prevent substantial modulation of amplitude over the whole body length.

There is also an interaction between h and swimming speed, as found for trout interacting with walls (Webb, 1993). For example, at 5 cm s^{-1} , P for plaice swimming with $h=10$ mm would have been 7.4 times that at $h=0$ mm. In contrast, at 45 cm s^{-1} , P was only three times larger at $h=10$ mm than at $h=0$ mm. Thus, the benefits of ground effects diminish as fish swim faster. This results from smaller downwash angles as speed increases (Reid, 1932; Lighthill, 1979).

The interactions between h and u on P may explain the modulation of tailbeat frequency in plaice swimming at the bottom compared with fish swimming at greater heights. Presumably, because of the greater importance of the ground effect at low speeds, plaice swimming at the bottom were able to produce sufficient thrust and lift with lower tailbeat frequencies. However, as speed increases, the ground effect diminishes and resistance increases, requiring proportionately higher tailbeat frequencies.

Symbols

10-min u_{crit}	10 min critical swimming speed
B	span, the depth of the body and fins
B_{\max}	maximum span
B_x	local span
c	backward speed of the propulsive wave
F	tailbeat frequency
F_x	local tailbeat frequency (equal to F)
H	amplitude of a tailbeat
h	height of the thin wire grid above the bottom, swimming height
H_x	local amplitude
L	total length of a fish
M	added mass per unit length of an element
P	mean rate of working
P_x	mean rate of working for an element at x
u	swimming speed
u_p	penultimate swimming speed before failure in the calculation of u_{crit}
W	mean lateral speed assuming sinusoidal motion
w	velocity given to the water
x	position along the body centerline

z	gap, the space between a solid surface and the thrust-producing body and fins
z/B	gap/span ratio
z/B_{\max}	gap/span ratio at the maximum span
$z_{1,\text{boat}}$	distance below the boat at one extreme of the tailbeat
$z_{1,\text{bottom}}$	distance above the bottom (ground) at one extreme of the tailbeat
$z_{2,\text{boat}}$	distance below the boat at the other extreme
$z_{2,\text{bottom}}$	distance above the bottom at the other extreme
z_{tail}/B	gap/span ratio for the tail
Δt	time between current speed increments
Δu	current speed increment
λ	length of propulsive wave
ρ_{water}	density of sea water

Support was provided by NSF grants IBN 9507197 and IBN 9973942. I thank the staff at the Lowestoft CEFAS laboratory, especially Dr G. P. Arnold and J. Metcalfe for the providing facilities and assistance.

References

- Anderson, D. F. and Eberhardt, S. (2001). *Understanding Flight*. New York: McGraw-Hill.
- Arnold, G. P. (1969). The reactions of plaice (*Pleuronectes platessa*) to water currents. *J. Exp. Biol.* **51**, 681–697.
- Arnold, G. P. and Weihs, D. (1978). The hydrodynamics of rheotaxis in the plaice (*Pleuronectes platessa*). *J. Exp. Biol.* **75**, 147–169.
- Bainbridge, R. (1963). Caudal fin and body movement in the propulsion of some fish. *J. Exp. Biol.* **40**, 23–56.
- Bartol, I. K., Mann, R. and Petterson, M. R. (2001a). Aerobic respiratory costs of swimming in the negatively buoyant brief squid *Lolliguncula brevis*. *J. Exp. Biol.* **204**, 3639–3653.
- Bartol, I. K., Petterson, M. R. and Mann, R. (2001b). Swimming mechanics and behavior of the shallow-water brief squid *Lolliguncula brevis*. *J. Exp. Biol.* **204**, 3655–3682.
- Blake, R. W. (1979). The energetics of hovering in the mandarin fish (*Synchropus picturatus*). *J. Exp. Biol.* **82**, 25–33.
- Blake, R. W. (1983a). *Fish Locomotion*. Cambridge: Cambridge University Press.
- Blake, R. W. (1983b). Mechanics of gliding birds with special reference to the influence of ground effect. *J. Biomech.* **16**, 649–654.
- Breder, C. M. (1926). The locomotion of fishes. *Zoologica* **4**, 159–297.
- Brett, J. R. (1964). The respiratory metabolism and swimming performance of young sockeye salmon. *J. Fish. Res. Bd. Can.* **21**, 1183–1226.
- Duthie, G. G. (1982). The respiratory metabolism of temperature-adapted flatfish at rest and during swimming activity and the use of anaerobic metabolism at moderate swimming speeds. *J. Exp. Biol.* **97**, 359–373.
- Gray, J. (1933). Studies in animal locomotion. I. The movement of fish with special reference to the eel. *J. Exp. Biol.* **10**, 88–104.
- He, P. and Wardle, C. S. (1986). Tilting behavior of the Atlantic mackerel, *Scomber scombrus*, at low swimming speeds. *J. Fish Biol.* **29** (Suppl. A), 223–232.
- Hoerner, S. F. (1975). *Fluid-dynamic Lift*. Brick Town, NJ: Hoerner Fluid Dynamics.
- Lighthill, J. (1975). *Mathematical Biofluidynamics*. Philadelphia: Society for Industrial and Applied Mathematics.
- Lighthill, J. (1979). A simple fluid-flow model of ground effect on hovering. *J. Fluid Mech.* **93**, 781–797.
- Moyle, P. B. and Cech, J. J. (1996). *Fishes: an Introduction to Ichthyology*. Upper Saddle River: Prentice Hall.
- Newman, J. N. and Wu, T. Y. (1973). A generalized slender-body theory for fish-like forms. *J. Fluid Mech.* **57**, 673–693.
- Norberg, U. M. (1990). *Vertebrate Flight*. New York: Springer-Verlag.
- Reid, E. G. (1932). *Applied Wing Theory*. New York: McGraw-Hill.

- Rosenberger, L. J.** (2001). Pectoral fin locomotion in batoid fishes: undulation versus oscillation. *J. Exp. Biol.* **204**, 379–394.
- Sokal, R. R.** (1995). *Biometry: The Principles and Practices of Statistics in Biological Research*. New York: Freeman.
- Videler, J. J.** (1993). *Fish Swimming*. New York: Chapman & Hall.
- Webb, P. W.** (1975). Hydrodynamics and energetics of fish propulsion. *Bull. Fish. Res. Bd. Can.* **190**, 1–159.
- Webb, P. W.** (1981). The effect of the bottom on the fast start of a flatfish, *Citharichthys stigmaeus*. *Fish. Bull.* **79**, 271–276.
- Webb, P.** (1988). 'Steady' swimming kinematics of tiger musky, an esociform accelerator, and rainbow trout, a generalist cruiser. *J. Exp. Biol.* **138**, 51–69.
- Webb, P. W.** (1989). Station holding by three species of benthic fishes. *J. Exp. Biol.* **145**, 303–320.
- Webb, P. W.** (1992). Is the high cost of body/caudal fin undulatory propulsion due to increased friction drag? *J. Exp. Biol.* **162**, 157–166.
- Webb, P. W.** (1993). The effect of solid and porous channel walls on steady swimming of steelhead trout *Oncorhynchus mykiss*. *J. Exp. Biol.* **178**, 97–108.
- Webb, P. W.** (2002). Control of posture, depth and swimming trajectories of fishes. *Integr. Comp. Biol.* (in press).
- Webber, D. M., Boutilier, R. G., Kerr, S. R. and Smale, M. J.** (2001). Caudal differential pressure as a predictor of swimming speed of cod (*Gadus morhua*). *J. Exp. Biol.* **204**, 3561–3570.
- Wilga, C. D. and Lauder, G. V.** (1999). Locomotion in the sturgeon: function of the pectoral fins. *J. Exp. Biol.* **202**, 2413–2432.
- Wilga, C. D. and Lauder, G. V.** (2000). Three-dimensional kinematics and wake structure of the pectoral fins during locomotion in leopard sharks, *Triakis semifasciata*. *J. Exp. Biol.* **203**, 2261–2278.
- Wilga, C. D. and Lauder, G. V.** (2001). Functional morphology of the pectoral fins in bamboo sharks, *Chiloscyllium plagiosum*: benthic vs. pelagic station-holding. *J. Morph.* **249**, 195–209.
- Wilkinson, L.** (1987). *SYSTAT: The System for Statistics*. Evanston, IL: SYSTAT.
- Wu, T. Y.** (1977). Introduction to scaling of aquatic animal locomotion. In *Scale Effects of Animal Locomotion* (ed. T. J. Pedley), pp. 203–232. New York: Academic Press.